

Effect of co-firing coal and biomass blends on the gaseous environments and ash deposition during pilot-scale oxy-combustion trials

N. Jurado ^a, N.J. Simms ^b, E. J. Anthony ^a, J. E. Oakey ^{b*}

^a Centre for Combustion, Carbon Capture and Storage, Cranfield University, Cranfield, Bedfordshire MK43 0AL, UK

^b Centre for Power Engineering, Cranfield University, Cranfield, Bedfordshire MK43 0AL, UK

* Corresponding author. E-mail address: J.E.Oakey@cranfield.ac.uk (J. E. Oakey).

HIGHLIGHTS

- Air- and oxy-combustion tests were carried out using El Cerrejon coal and biomass (cereal co-product) in a 100 kW_{th} pilot combustor
 - Co-firing tests were carried out using coal with biomass additions of 25 and 50% (w/w)
 - Increasing the share of cereal co-product reduced SO₂ and increased HCl levels in the flue gas
 - Sulphur levels were similar in deposits from oxy-firing 100% El Cerrejon and 100% cereal co-product due to K₂SO₄ formation
 - Chlorine was only found in the deposits generated from oxy-firing 100% cereal co-product
-

ABSTRACT

This paper presents the experimental results from co-firing blends of El Cerrejon (EC) coal and cereal co-product (CCP) using several ratios (100/0; 75/25; 50/50; 0/100 (w/w)) under air- and oxy-firing conditions, in a retrofitted 100 kW_{th} pulverised fuel combustor. An on-line high-resolution multi-component Fourier Transform Infra-red (FTIR) analyser was used to measure CO₂, O₂, H₂O, CO, NO, NO₂, N₂O, NH₃, SO₂, HCl, HF and CH₄. A comprehensive evaluation of the major and minor species present in the flue gas was carried out to study the effects of the addition of biomass, the firing mode (air/oxy) and the type of recycle (wet/dry) on the gaseous environment in the combustor. It was found that similar CO₂ levels can be reached when using pure coal or pure biomass, on a dry basis. For the minor species, the increase in the share of biomass had the effect of decreasing the SO₂ levels reached in the flue gas and increasing the HCl content. No significant variation in the NO_x levels was observed as a consequence of using high percentages of biomass. For ash deposit characterisation, two probes were used for which surface temperatures were controlled at 650° and 750°C. Environmental scanning electron microscopy (ESEM) with energy dispersive X-ray (EDX) analysis, supported by X-ray diffraction (XRD), were used to study the deposits. The ESEM/EDX and XRD results showed similar sulphur levels in the deposits when varying the share of biomass even though EC coal contains 3.5 times more sulphur than CCP. This is thought to be a consequence of the reaction of sulphur with the alkalis, especially potassium, present at higher levels in the CCP, which produces higher levels of K₂SO₄ in the combustion gas. Chlorine was only found in the deposits generated using pure CCP under oxy-firing conditions. An evaluation of the different mineral species formed when varying the biomass share and the firing mode was also performed. Results obtained comparing the mineral species in deposits when using 100% CCP, switching from air to oxy-firing conditions, showed that in air-firing CCP deposits had higher levels of aluminium phosphate and arcanite (K₂SO₄). Also, under oxy-firing conditions, 100% CCP-derived deposits had a higher level of potassium magnesium chloride compared 100% EC.

Keywords:

Oxy-fuel

Co-firing

Coal combustion

Biomass

Ash deposition

Alkali sulphates

1. Introduction

43 The production of energy represents the largest contribution to anthropogenic greenhouse gas emissions,
44 accounting for 83% of the total, followed by agriculture (8%), industrial processes (6%), and waste (3%) [1]. Figures
45 reported in 2013[1] by the International Energy Agency (IEA) showed that although coal represented 29% of the
46 primary energy supply, the use of coal was responsible for the highest fraction of the global CO₂ emissions (44%),
47 followed by oil (35%), and gas (20%); only 1% of the share of CO₂ emissions was due to the use of carbon-neutral
48 fuels, where nuclear, hydro, geothermal, solar, tide, wind, biofuels and waste are included. Coal is the highest
49 contributor to CO₂ emissions because of its high content of carbon per unit of energy released, and the fact that energy

49 from carbon-neutral fuels accounted for only 18% of energy production in 2011. These figures together with the UK
50 target to reduce its carbon emissions by 80% from 1990 levels by 2050 [2], and the need for flexible power, mean that
51 carbon capture and storage (CCS) technologies and biofuels must play an important role to achieve the goals set by
52 2050 in UK.

53 The CCS option studied here is based on oxy-combustion. In this technology, the fuel is fired in an oxygen-
54 enriched environment with a reduced level of N₂ to generate a flue gas with high concentration of CO₂. Part of the flue
55 gas is recirculated to the combustor to replace the air-derived N₂ missing in oxy-firing and control flame temperature.
56 The exhaust gas exiting the process needs a less energy intensive treatment, in comparison to other post-combustion
57 technologies, to reach the CO₂ purity needed to be storage ready. The compression and purification unit (CPU)
58 operates downstream of the typical gas treatment required in air-firing combustion (deNO_x, deSO_x and ESP), and
59 consists of the further purification of the CO₂ stream, during and after compression. The supercritical fluid phase
60 product stream from the CPU, typically has a CO₂ purity of 95% (v/v) or higher [3]. Despite the promise of oxy-
61 combustion with coal and biomass co-firing, improved understanding of the environment inside the oxy-combustor,
62 heat transfer, characteristics of the ash deposits or materials corrosion behaviour is still required through further study.

63 The use of biomass for co-combustion requires the evaluation of its composition and properties, as well as the
64 assessment of industrial and environmental implications of co-firing it with coal [4]. Vassilev et al. [4] highlighted the
65 importance of characterising biomass in terms of its: (i) chemical composition (i.e., major and minor substance as
66 well as trace elements); (ii) mineral composition, considering organic matter (e.g., cellulose, hemicellulose, lignin,
67 char, etc.), and inorganic matter; and (iii) other properties (i.e., volatile matter, fixed carbon, moisture, ash content,
68 ash-fusion and combustion temperatures, density, pH, calorific value, etc.). Unfortunately in many cases such
69 information is not available; however, it is known that:

- 70 – Char reactivity is higher when using biomass in comparison with that of coal and biomass has a higher
71 volatile content. This allows ignition of the char to be achieved at lower temperatures, and so less power
72 is required for start-up of the combustion of the fuel. Namely, decreasing ignition temperatures have
73 been seen with increasing share of biomass in the fuel mix under oxy-firing conditions [5,6].
- 74 – Burnout. The degree of burnout might be expected to be enhanced for coal/biomass blends due to the
75 higher volatile content of the biomass; however, Arias et al. [5] suggested that this increase is almost
76 negligible. Other studies have shown that burnout when co-firing is improved by the use of biomass, and
77 have suggested this to be a consequence of two effects: (i) the higher volatile content and reactivity of
78 the biomass-derived char as mentioned above, and (ii) higher oxygen content in biomass, which
79 increases the char oxidation rate [7].
- 80 – Heat flux. A few studies have been carried out on the effect on the heat transfer due to the change in the
81 environment composition inside the reactor when oxy-firing coal and/or biomass [7,8]. Smart et al. [7]
82 suggested that even though peak radiative and convective heat fluxes similar to the air-firing case can be
83 obtained under oxy-firing conditions using coal or coal/biomass blends, they do not occur at the same
84 operating conditions (e.g., flue gas recycle ratio), or at the same location (i.e., distance from the burner),
85 because they are fuel dependent. The industrial implication of this can be that optimal operation cannot
86 be reached for retrofitted plants as the superheaters and reheaters would be characterised based on a coal-
87 based design; and that for new-build plants it may be necessary to redesign the superheaters and
88 reheaters.

89 Regarding the environmental challenges of using biomass as fuel for power generation, both positive and negative
90 aspects reported [4], highlighting that a complete biomass life cycle assessment is a very important tool, necessary to
91 conduct a proper evaluation of its use. Consequently, it is advised that the biofuels employed should be classified as
92 whether they are sustainable or represent unsustainable management resources, to avoid serious environmental
93 problems [4].

94 One important characteristic of the ash generated under oxy-combustion conditions is the higher likelihood that
95 corrosion problems will appear in the boiler when fuels with medium and high content of S, Cl, and F are used,
96 because of the changed environment arising from flue gas recycle. This recycle leads to the accumulation of these
97 species inside the combustor. This, combined with greater sulphur oxides retention in fly ash when burning blends of
98 coal and biomass, due to higher alkali content in biomass [6,9–13], can cause an increased risk of corrosion as
99 reported by Syed et al. [9]. In their paper, it was concluded that more corrosion damage occurs under oxy-firing
100 conditions of coal and biomass blends in comparison to air-firing combustion. The propensity to form ash deposits, as
101 well as slagging and fouling issues related to the use of biomass in thermal applications have been addressed by
102 several authors [10–12]. Khodier and Simms [10] pointed out the influence of Na₂SO₄ in the formation of a sticky,

103 adhesive layer at the onset of deposit formation when co-firing with air. However, Chen et al. [12] noted in their paper
104 that there is a lack of literature on the behaviour of ash, mechanisms of slag layer formation and its interaction with
105 char particles, under oxy-combustion conditions.

106 In this work, experimental tests were performed co-firing a South American coal, El Cerrejon (EC), and a form of
107 processed biomass, cereal co-product (CCP), under oxy-firing conditions using a retrofitted 100kW_{th} pulverised coal
108 combustor facility at Cranfield University. Tests using air combustion were also carried out to establish the reference
109 case. A parametric study was performed with respect to the effect of fuel variability on composition of the combustion
110 gas and ash deposits, paying special attention to the fate of sulphur, a key component regarding corrosion. The
111 biomass composition, specifically its alkali and alkaline earths content, has been observed to be an important factor
112 with regard to sulphur retention in ash deposits or conveyed in the gaseous phase as alkali sulphate aerosols. The
113 higher potential for alkali species, K in particular [13], to react with SO₃ to form sulphates by nucleation when flue
114 gases are cooled down to around 1150K, was studied by Jiménez and Ballester [14]. These authors found that when
115 burning pure biomass or co-firing it with coke, K₂SO₄ appeared to be the only major compound in the submicron
116 particles. Research focused on the use of biomass (pure or co-fired) to analyse the generation of alkali sulphates in
117 conventional combustion has been done, e.g., the aforementioned work [14], or the studies carried out by Valmari [15]
118 and Kassman et al. [16]. These studies were, for the most part, carried out by doping the biomass with S for the K (or
119 other alkalis present) to react with it instead of with the Cl also present in the biomass, because KCl presents more
120 corrosion problems than K₂SO₄. Other authors have measured SO₃ levels [17] or quantified the release of alkali
121 sulphates [18] when oxy-firing coal. Modelling work, using density functional theory calculations, has also been
122 carried out by Galloway et al. [13] with regard to SO₃ retention in fly ashes, specifically its tendency to form bonds to
123 certain species, such as CaO, MgO, Na₂O or K₂O, concluding that the higher binding strengths are associated to
124 potassium. Nonetheless, little work has been published on experimental studies of alkali sulphate levels combining
125 both options: co-firing coal and biomass under oxy-firing conditions, which is one of the main purposes of the study
126 reported here.

127 **2. Experimental procedure**

128 *2.1 Pilot-scale combustion test facility*

129 The experiments were conducted in the 100 kW_{th} pilot-scale pulverised fuel combustion facility at Cranfield
130 University. A schematic diagram of this facility configured for oxy-combustion is shown in Fig. 1.

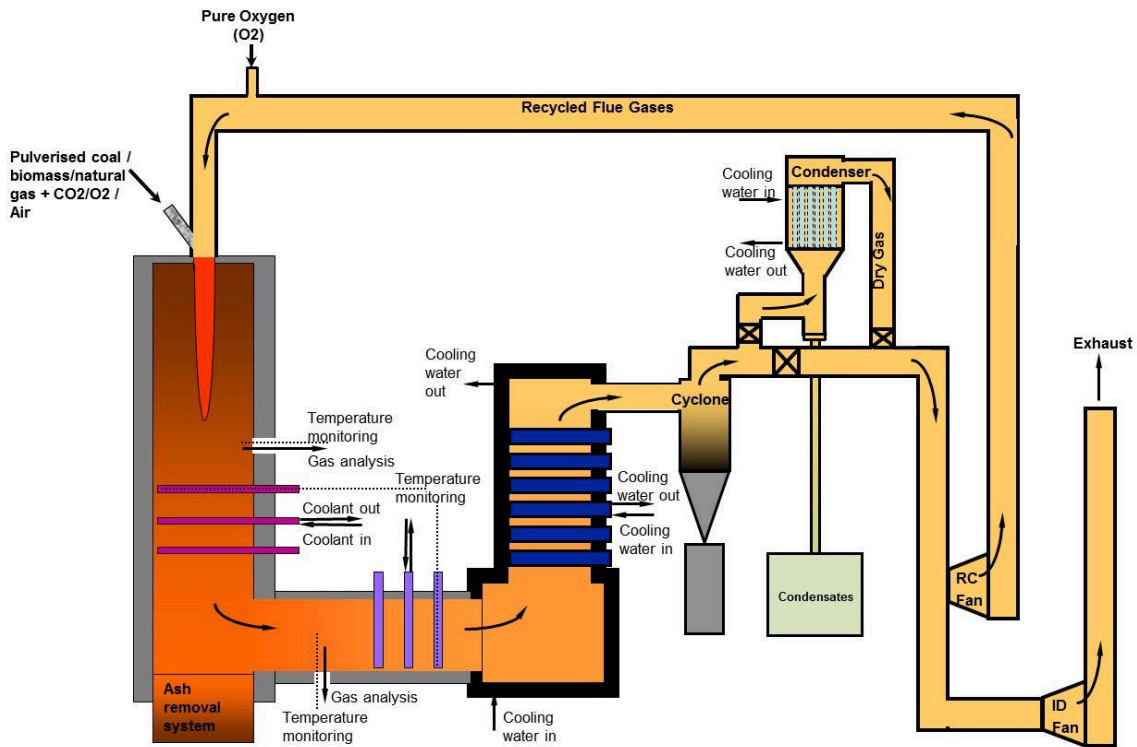


Fig. 1. Schematic diagram of the pilot-scale (100 kW_{th}) pulverised fuel oxy-combustion facility at Cranfield University.

The pulverised fuel was fed to the oxy-combustor at a constant rate using a fuel feeder provided by a metering screw, a vibratory tray and a venturi eductor. Additionally, the feeder has three purge points where CO₂ is injected to keep a positive pressure inside the pulverised fuel feeding system so as to avoid air ingress. Once the pulverised fuel reaches the venturi eductor, it is entrained and conveyed to the burner by a stream of pure CO₂ gas coming from CO₂ cylinders. Prior to this stream being fed to the burner, the primary O₂, coming from O₂ cylinders, was injected into the stream, when using this option (primary O₂) for a particular test. A secondary oxygen stream was used for all the oxy-firing tests, and was injected into the flue gas recycle path 1.5 m before its entrance to the oxy-combustor, as can be seen in Fig. 1.

The combustor was equipped with a down-fired burner, provided with a pilot flame port and a flame detector. The pulverised fuel was combusted in the vertical combustion chamber (3.7 m height) which has a square cross-section with sides of 650 mm surrounded by thermal insulation (175 mm thickness). The vertical combustion chamber has four view ports and ports where sensors are used to measure wall temperatures (three R type and three K type thermocouples). Three of the sampling ports, located at the bottom part of the vertical section, are used to locate 'radiant' deposition probes. To collect the deposits, it was necessary to allow the chamber to cool down for 18 to 24 h. Then the ash deposited on the probes was sampled and analysed using ESEM/EDX and XRD techniques (see next subsection 2.2.1 for further description of ash deposit analysis). An on-line high-resolution multi-component Fourier Transform Infra-red (FTIR) analyser was used to measure CO₂, O₂, H₂O, CO, NO, NO₂, N₂O, NH₃, SO₂, HCl, HF and CH₄ (see previous work in this facility [19] for a more detailed description of this method). Special calibration spectra for 28 gas species were produced and loaded onto the FTIR sensor to measure gas emissions generated under oxy-combustion conditions, as a consequence of the different ranges for concentrations expected, especially for water vapour and CO₂, for which upper detection levels needed to be upgraded. The primary sampling point for the FTIR analyser was located in the vertical section of the combustor, in a port above the ones used for the ash deposit probes. A secondary FTIR sampling point was positioned after the condenser, to be able to quantify the efficiency of the condenser in removing water and soluble species.

Part of the exhaust gas was recirculated to the combustion chamber, through the recycle (RC) fan, and the remainder was sent to the stack, through the induced draft (ID) fan. The lines that convey the recycled flue gas are thermally insulated and have a trace heating system to avoid the temperature dropping below the acid dew point of the flue gas. Secondary O₂ was injected into this stream prior to feeding it to the oxy-combustor. A secondary analyser, an ADC MGA 3000 Multi Gas Analyser which measures CO₂, CO, O₂ and SO₂, sampled the gas just before its entrance

162 into the burner to monitor that the percentage of oxygen was in the range specified (27-35% v/v) for the oxy-firing
163 tests.

164 2.2 Ash sampling and analysis techniques

165 2.2.1 Deposit probes

166 Deposit samples from the early stages of ash deposition were collected using ceramic sections mounted on
167 metallic air-cooled probes, which were located in the lower part of the vertical section of the combustor radiant zone.
168 These probes were placed perpendicularly to the direction of the flue gas flow. For all the tests, the nominal average
169 surface temperatures of the probes were maintained at 650 and 750°C, respectively, to simulate the surface
170 temperatures reached at the superheaters/reheaters, by using cooling compressed air supplied to the internal body of
171 the probe.



172
173 **Fig. 2. Deposition probe**

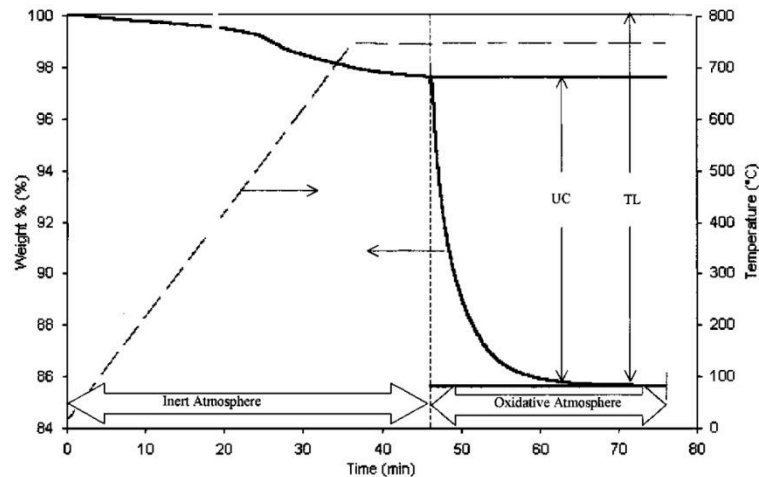
174 The compositions of the sampled deposits were analysed using two different techniques: environmental scanning
175 electron microscopy (ESEM) with energy dispersive X-ray (EDX), and X-ray diffraction (XRD). The ESEM/EDX
176 analysis provides information about the elements present on the surface of the sample, while XRD analysis is
177 particularly recommended for crystalline samples, providing information about existing chemical compounds, but is
178 less effective for amorphous materials. Most of the deposit structure is amorphous, so the main technique to evaluate
179 the deposit composition was the ESEM/EDX. However, while most of the deposit material would be expected to be
180 amorphous, the XRD technique was useful in characterising the crystalline compounds present in the deposits.

181 2.2.2 Fly ash

182 As part of the studies carried out for this work, the amounts of unburnt carbon present in the fly ash samples
183 collected from the oxy-combustion process were evaluated. Fly ash was collected from two locations: the horizontal
184 section of the combustor and the cyclone. For the evaluation of unburnt carbon in ash, the loss on ignition (LOI)
185 method can be applied [20]; although some studies [21] have suggested that the results for remaining char content
186 using the LOI technique should be analysed with caution when evaluating fly ash enriched in calcium at temperatures
187 above 500°C, and that the use of additional techniques is advised for such cases. For the LOI method, the LOI at
188 550°C (LOI550) is related to the organic carbon content of the sample, and the LOI at 950°C is associated with the
189 inorganic carbon content according to Santisteban et al. [20]. Other studies [22,23] have demonstrated that the LOI
190 method overestimates the unburnt carbon for coal and biomass ash, respectively, when there are volatile compounds
191 ,organic or inorganic, that can contribute to the weight loss measured during the analysis, but which are not related to
192 residual carbon present in the sample. In the study carried out by Fan and Brown [22], where coal was used, the
193 authors reported an overestimation around 20%. Zhao et al. [23] studied the characteristics of ash generated from
194 burning biomass, stating that the positive bias given by LOI550 is due to the effect of release of VOCs in the ash, and
195 also, because at the ashing temperature, a small amount of carbonates may decompose, contributing to the weight loss.
196 The presence of carbonates in the fly ash generated under oxy-firing conditions has been suggested by Wigley [24] to
197 be a consequence of the inhibited decomposition of carbonates, present as minerals in the original fuel, at the high
198 partial pressures of CO₂ in the oxy-combustion environment. Zhao et al. [23] suggested measuring the carbon in ash
199 by thermogravimetric analysis (TGA). In addition to these techniques, which belong to the ashing procedures, there is
200 a wide range of methods that can be applied to study the organic and inorganic matter present in fly ash, according to
201 Vassilev et al. [21]. These procedures can be classified into: (i) ashing procedures (i.e., high and low-temperature
202 ashing); (ii) physical separation (e.g., by density, by size, magnetically, electrostatically, etc.); (iii) chemical leaching
203 (i.e., dissolution of organic/inorganic matter, sequential leaching); (iv) sequential physical and chemical separations.

204 The selection of the method(s) to evaluate the organic and inorganic matter of the fly ash will depend on several
205 factors, such as: accuracy required of the analyses results, resources available (i.e., accessibility to equipment or
206 qualified personnel, time availability), etc.

207 The technique used here to measure the carbon content of the fly ash for this work was a modification of TGA
208 using consecutive inert and oxidising atmospheres and based on the literature this seems to be an adequate method
209 [22,23]. In the variation used for the present work, the sample's weight is not measured during the process, but rather
210 at the beginning, after passing one hour in an inert-atmosphere (N_2) furnace at $750^\circ C$, and after passing one hour in an
211 oxidizing-atmosphere (air) furnace at $750^\circ C$. In the first stage, the sample is heated in an inert atmosphere (N_2),
212 liberating the volatile matter. Then, the ash is exposed to an oxidising atmosphere, to cause the unburnt char carbon to
213 react. The weight of the sample is recorded during the entire TGA experiment, producing a curve similar to the one
214 shown in Fig. 3, where UC denotes unburnt carbon, and TL denotes total loss.



215

216

Fig. 3. TGA weight loss curve of a typical fly ash sample. Image taken from Fan and Brown [22]

217 2.3 Fuels

218 The fuels used for this study, EC and CCP, were supplied by E.ON New Build and Technology Ltd. (Power
219 Technology Centre, Ratcliffe-on-Soar, Nottingham, UK) to the OxyCAP-UK consortium, funded by UK
220 Engineering and Physical Sciences Research Council (EPSRC) where all the academic partners, Cranfield
221 University amongst them, were studying the same fuels in order to generate comparable results. Both fuels were
222 supplied in a pulverised form. The CCP used for this work is a blend of agricultural sub-products, produced from
223 wheat, and straw briquettes. To avoid problems related to blockages in the eductor in the fuel feeding system,
224 biomass was sieved before each test using a 2 mm mesh size, which gave an average particle size of 0.5 mm.
225 Constant pulverised fuel flowrates of 13.5, 15, 16.7 and 22 kg/h were supplied to the oxy-combustor with CCP
226 additions of 0, 25, 50, and 100% (w/w), respectively.

227 Table 1 shows the proximate, ultimate and ash analyses of the fuels used for this study. The higher content of
228 moisture and volatile matter of the CCP, as well as the higher levels of oxygen, hydrogen, nitrogen and chlorine in
229 comparison to the levels presented for EC can be seen. By contrast, EC coal presents a higher level of ash in its
230 proximate analysis and considerably higher calorific value than CCP. Also noteworthy are the high levels of K_2O
231 and P_2O_5 in the CCP ash analysis.

232 Table 1. Proximate, ultimate, mineral and ash analyses of the fuels.

	El Cerrejon coal	Cereal co-product
Proximate analysis (% (w/w) as received)		
Moisture	5.80	8.10
Volatile matter	34.80	70.80
Ash	8.60	4.20
Calorific value, (MJ/kg)		
Gross calorific value	27.85	17.61
Net calorific value	27.12	16.34
Ultimate analysis (% (w/w) as received)		
Carbon	69.2	43.30
Hydrogen	4.40	5.80
Nitrogen	1.42	2.70
Chlorine	0.02	0.17
Sulphur	0.58	0.16
Oxygen	9.98	35.57
Mineral analysis (% (wt))		
Kaolinite $\text{Al}_4\text{Si}_4\text{O}_{10}(\text{OH})_8$	16.80	-
Illite $\text{KAl}_2(\text{OH})_2(\text{AlSi}_3\text{O}_{10})$	9.40	-
Pyrite FeS_2	12.90	-
Quartz SiO_2	54.20	-
Coquimbite $\text{Fe}^{-3}_2(\text{SO}_4)_3 \cdot 9\text{H}_2\text{O}$	3.50	-
Bassanite $\text{CaSO}_4 \cdot 0.5\text{H}_2\text{O}$	3.20	-
Ash analysis (% (w/w))		
SiO_2	60.69	44.36
Al_2O_3	22.01	2.79
Fe_2O_3	7.43	2.47
TiO_2	0.92	0.12
CaO	2.27	7.78
MgO	2.90	3.96
Na_2O	1.06	0.36
K_2O	2.32	24.72
Mn_3O_4	0.06	0.10
P_2O_5	0.21	12.04
SO_3	-	-
BaO	0.11	0.05

233 The size distribution of the fuels used is presented in Table 2.

234 Table 2. Size distribution of fuels (wt% in size class)

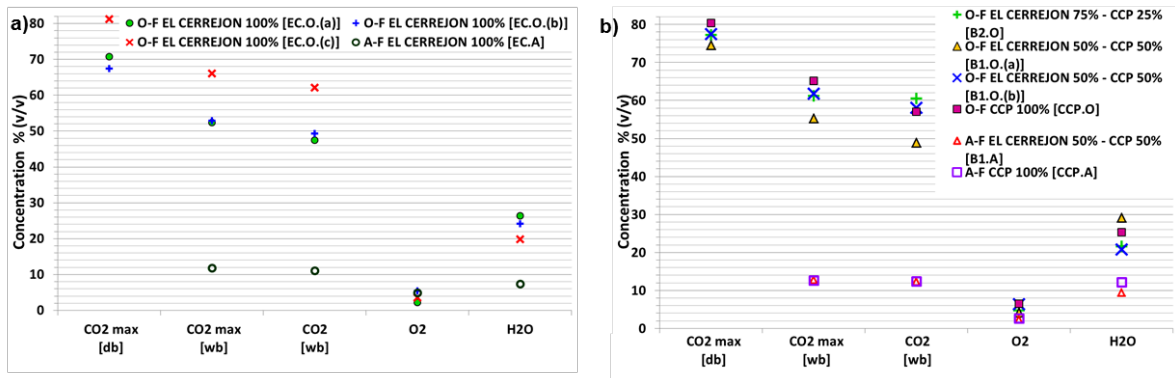
Size (μm)	El Cerrejon coal (EC)	Cereal co-product (CCP)
10	-	0.06
30	0.40	6.38
50	1.23	9.48
70	5.04	9.94
90	6.12	14.63
110	6.52	-
130	7.15	29.40
150	4.73	30.11
170	15.99	-
190	0.24	-
210	12.97	-
230	39.61	-

235 **3. Results and discussion**

236 **3.1 Gaseous environments**

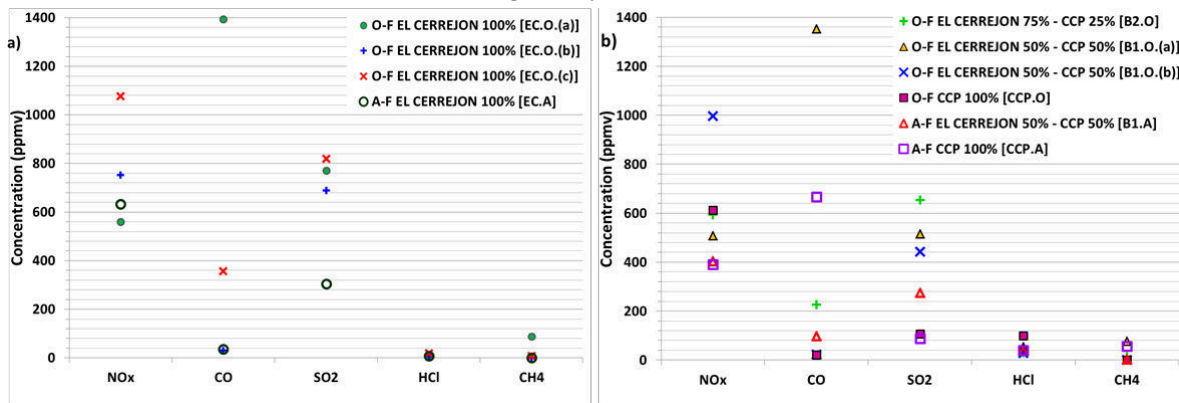
237 **3.1.1 Effect of co-firing on gaseous environment**

238 The mean values for the gaseous species for various fuel compositions (blends of EC with 0, 25, 50 and 100%
 239 (w/w) of CCP) are presented in Fig. 4 for the major species and in Fig. 5 for minor species, under air and oxy-firing
 240 conditions. The cases using coal are shown in the sub-figures denoted a), while the co-firing cases are denoted with b).



241 **Fig. 4 Gaseous environments - major species; a) coal only, b) coal-CCP co-firing**

242 [EC: El Cerrejon coal; CCP: Cereal co-product; B1: Blend EC50/CCP50; B2: Blend EC75/CCP25; A-F: Air-firing; O-F: Oxy-
 243 firing; db: dry basis; wb: wet basis]

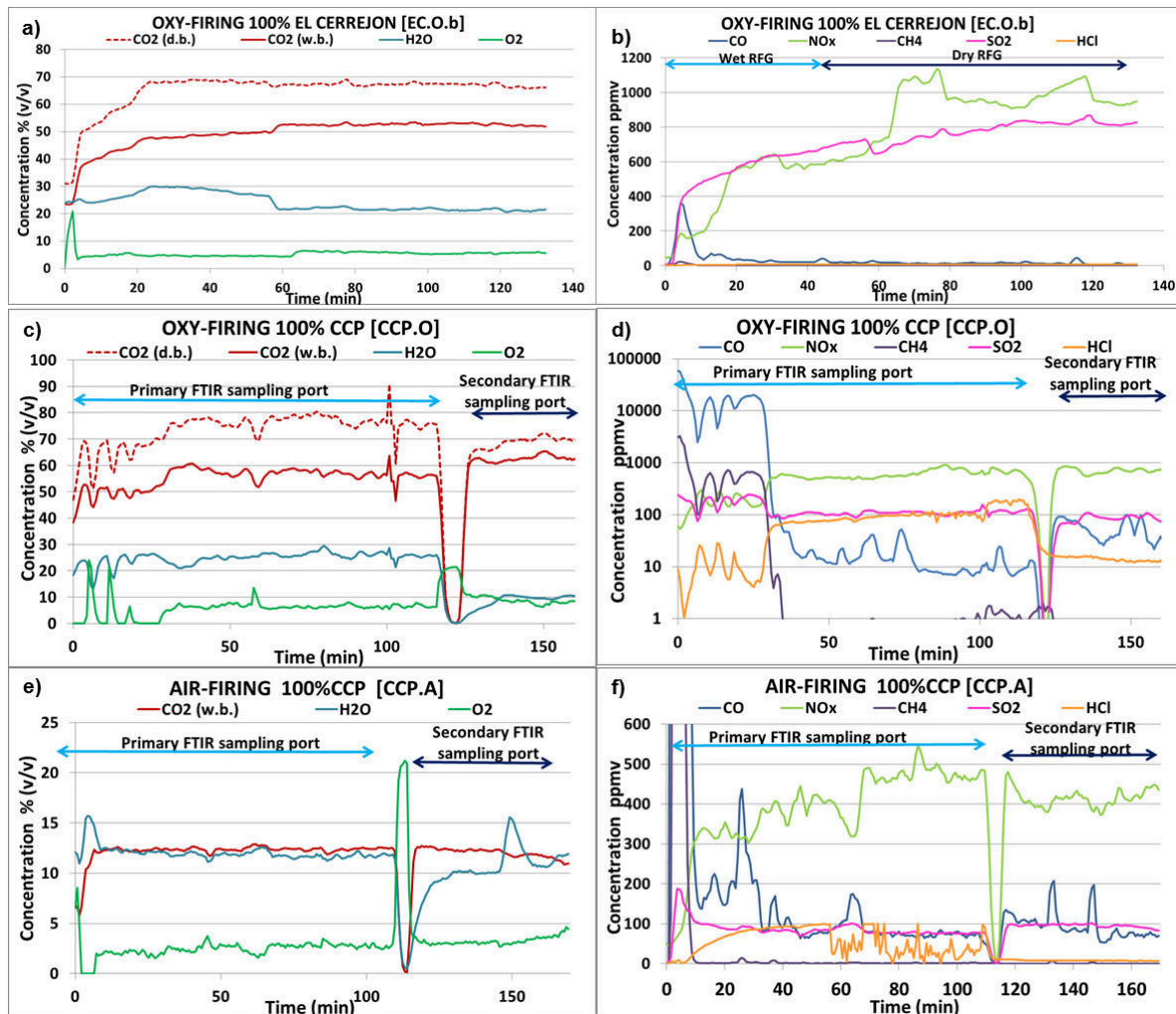


244 **Fig. 5 Gaseous environments - minor species; a) coal only, b) coal-CCP co-firing**

245 [EC: El Cerrejon coal; CCP: Cereal co-product; B1: Blend EC50/CCP50; B2: Blend EC75/CCP25; A-F: Air-firing; O-F: Oxy-
 246 firing; db: dry basis; wb: wet basis]

247
 248 The gas composition measured for the major species shows that the maximum CO₂ level reached, on a wet basis,
 249 occurs in the case of 100% coal [EC.O.(c)], as expected given the fuel analyses. Interestingly, similar values for the
 250 CO₂ levels on a dry basis were achieved when using both parent fuels, in tests [EC.O.(c)] and [CCP.O]. For the H₂O
 251 content, the high levels obtained are due to the fact that the condenser could not remove all the steam present in the
 252 flue gas prior to recycling. The efficiency of the condenser can be defined as the ratio (molar- or mass-basis) between
 253 the amount of the condensable species 'i' that condenses and is removed from the flue gas, after having been cooled
 254 down, and the amount of i that entered the condenser. The condenser efficiencies observed for water vapour during
 255 the experiments were: 33% for 100% El Cerrejon coal, 57% for blend B1 (EC50/CCP50), 53.5% for blend B2
 256 (EC75/CCP25), and 86% for pure cereal co-product. The average value for water vapour in the flue gas measured
 257 inside the combustion chamber was in the range of 20-25% (v/v), being the maximum for the case when using 100%
 258 CCP. The excess O₂ was between 3.5 and 6.5 % (v/v), in most cases. To help the discussion on the gas environments,
 259 Fig. 6 presents the evolution of the major and minor species for selected tests. For the minor species, the CO levels
 260 were usually under 100 ppm, but fluctuations occurred at the beginning of some of the tests, before reaching stable
 261 operation, which increased such mean values noticeably. This can be seen in Fig. 6 (d) and Fig. 6 (f) where CO peaks
 262 occurred within the first 40 minutes of operation, when the transient regime occurred. With regard to the NOx

263 concentrations, the general trend shows that there are no significant changes related to the variation of the fuel; for the
 264 oxy-firing tests, NO_x levels were in the range of 550-750 ppmv. The high NO_x concentration, reached in the case
 265 using pure coal [EC.O.(c)], may be explained by the NO_x thermal generation being promoted due to the high
 266 temperatures reached in that test. To explain the high NO_x reached in the case using 50% EC-50% CCP blend
 267 [B1.O.(b)] in which there was an excess of oxygen around 6% (v/v), previous work by other authors [25,26] should be
 268 considered. These previous studies reported that increasing the excess of oxygen supplied to the burner led to an
 269 enhancement of NO production from the fuel-N, which seems to be the situation for this test: high levels of O₂ and
 270 50% (w/w) of the share of CCP, which has more nitrogen in its composition than EC. The data reported for SO₂ levels
 271 agree with expectations when considering the fuel analyses: higher range (680-820 ppmv) in the tests using 100%
 272 coal, medium range (440-650 ppmv) for those tests using coal-biomass blends, and the lowest concentration (around
 273 100 ppmv) for the case using only biomass. Likewise, the levels measured inside the combustor for HCl also follow
 274 the trend set by the ultimate analysis of the fuels: increasing with the share of biomass.



275
 276 **Fig. 6 Gas composition for selected tests: (a) Major species oxy-firing 100% EC; (b) Minor species oxy-firing 100% EC; (c) Major**
 277 **species oxy-firing 100% CCP; (d) Minor species oxy-firing 100% CCP; (e) Major species air-firing 100% CCP; (f) Minor species**
air-firing 100% CCP

278 3.1.2 Effect of oxy-firing mode on exhaust gas

279 From the values reported in Fig. 5 and Fig. 6, the average gas composition obtained under air- and oxy-firing
 280 conditions can be compared. For the main species (CO₂, H₂O) – see Fig. 6 (c) and Fig. 6 (e) – and some minor species
 281 (SO₂, HCl) – see Fig. 6 (d) and Fig. 6 (f) – the effect of recycling flue gas is noticeable, causing the levels to increase
 282 to two to three times their values in comparison to the air-firing case using the same fuel; this is a consequence of the
 283 accumulation inside the process of the species that are not completely removed prior to the recirculation of the flue
 284 gas to the oxy-combustor. However, the NO_x levels remain similar for most cases; this means an actual decrease of
 285 NO_x emissions per unit of energy produced [27]. This observation is in agreement with results reported by Toftgaard

286 et al. [6] where NO_x emissions were stated to be significantly reduced under oxy-firing conditions due to the near
287 elimination of thermal NO formation and to re-burning of NO_x passed through the burners with the recycled flue gas.
288 Note that the higher concentrations of SO_2 levels inside the oxy-combustor, previously reported in subsection 3.1.1,
289 are not normalised per unit of energy released from the fuel; considering this normalisation the results also follow the
290 decreasing trends when using oxy-combustion mode in comparison to air-firing. This remark is consistent with what
291 has been reported in other studies looking at the impact of the firing mode, air vs. oxy, on the SO_x emissions. This
292 effect has been described as being small [6], or showing a decrease in the conversion from fuel-S to SO_2 [17,28] under
293 oxy-firing conditions levels, which was explained by Fleig et al.[28] to be a consequence of the higher SO_2
294 concentrations which favour the formation of sulfates.

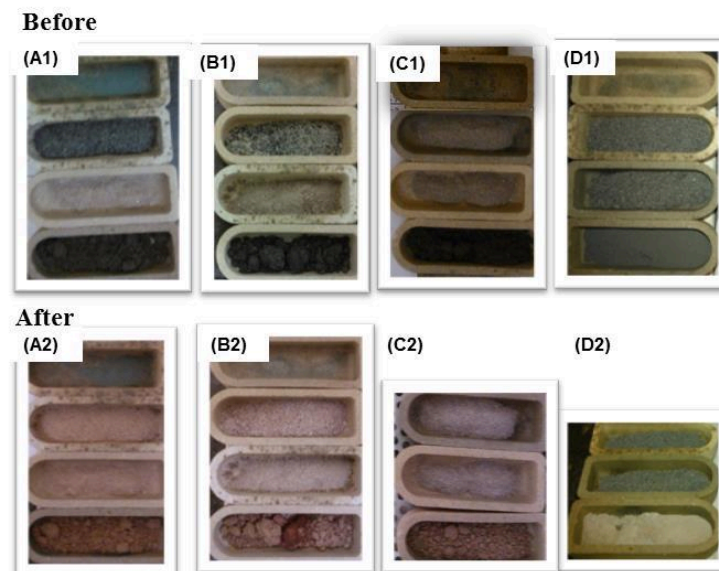
325 3.1.3 Effect of recycle type: wet vs. dry

326 As expected, all species increased in concentration except steam/water, as a consequence of changing the type of
327 recycle (from wet to dry). This effect can be seen in Fig. 6 (a) and Fig. 6 (b), towards minute 60, when the change in
328 the type of recycle was done during one of the oxy-firing tests. Fig. 6 (a) shows that there is an increase in CO_2 levels
329 and a decrease in H_2O of around 5-8% (v/v), with a less noticeable rise (around 3% higher) in oxygen concentration.
330 For the minor species, the effect of varying the type of recycle can be seen in Fig. 6 (b), particularly visible for the
331 NO_x concentration. The equivalent effect for SO_2 is less pronounced, presumably due to some SO_2 being extracted
332 with water in the condenser, leaving less in the recycled flue gas.

333 3.2 Ash behaviour

334 3.2.1 Fly ash characterisation

335 The fly ash was collected from two different locations: the horizontal section of the combustor (A) and the cyclone
336 (B). The aim of analysing these samples was to evaluate the unburnt carbon present in the ash settled during the tests,
337 to get a better understanding of whether the fuel used (coal/biomass/blends) or the firing mode (air/oxy-firing) had a
338 noticeable effect on the carbon burnout of the fly ash generated. Fig. 7 shows the crucibles containing the ashes
339 evaluated, before and after the unburnt carbon-in-ash tests. An empty crucible was used in all the tests, to identify any
340 systematic changes in measurements resulting from variations in the tests' environmental conditions, giving changes
341 in readings which were not due to the mass loss of the sample during the combustion process but were due to
342 differences from one day to another in environmental humidity, ambient pressure, etc.



343

344 **Fig. 7. Samples for unburnt carbon in ash from oxy-firing experiments before (1) and after (2) the burnout tests: (A) 100% EC; (B)**
345 **75% EC-25% CCP; (C) 50% EC-50% CCP; (D) 100% CCP**

346 The results obtained after performing the unburnt carbon-in-ash analyses using the technique already explained in
347 the experimental procedure (see subsection 2.2.2) are presented in Table 3.

318

Table 3. Unburnt carbon-in-ash results (%). Location A: Horizontal chamber; B: Cyclone319
320

[EC: El Cerrejon coal; CCP: Cereal co-product; B1: Blend EC50/CCP50; B2: Blend EC75/CCP25; A-F: Air-firing; O-F: Oxy-firing]

Sampling point	EC.A	B1.A	CCP.A	EC.O. (b)	EC.O. (c)	B1.O. (a)	B1.O. (b)	B2.O	CCP.O
A	31.4	-	-	-	43.5	-	-	30.5	-
B	38.3	33.2	30.0	9.4	7.4	11.4	16.2	8.9	8.3

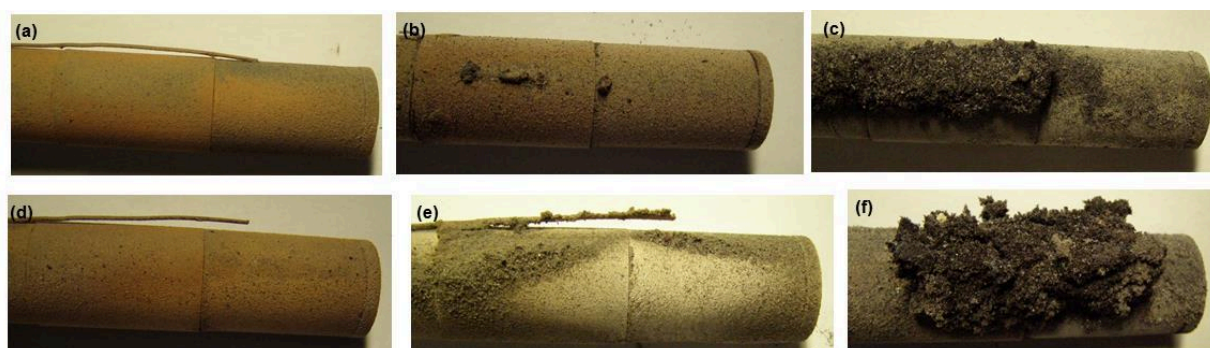
321 The unburnt carbon in the ash from the horizontal section of the combustor (denoted with A) is quite high in all
 322 cases, possibly due to incompletely burned fuel particles separating from the main gas flow. High levels are also
 323 found for the cyclone ash samples in all air firing cases. . However, there was significantly less unburnt carbon
 324 cyclone ash in the oxy-firing cases compared to air-firing, suggesting that combustion is continuing along the gas path
 325 between A and B under oxy-firing conditions, as a consequence of the higher temperatures and O₂ concentration for
 326 the oxy-firing tests. A further possible reason for the overall high levels in unburnt carbon observed in the fly ashes
 327 could relate to the particle size distributions of the fuels, with an excessive fraction of large particles, in which EC was
 328 supplied, as can be seen in Table 2.

329

3.2.2 Deposit characterisation

330 The ash deposits formed after approximately 3h of steady operation are presented in Fig. 8. It can be seen that the
 331 amounts of deposit generated for the cases when using pure biomass are noticeably higher than for the cases using
 332 pure coal or coal/biomass blends. Another observation is that changing the firing mode does not seem to have as great
 333 an effect on deposit build-up as varying the fuel blend. This fact has been previously observed by other authors [19]
 334 and identified as a consequence of the higher alkali content of biomass fuels, such as CCP, resulting in stickier
 335 particles, leading to softer, lower-density deposits, thus raising the rate of deposit build-up. The high content of alkalis
 336 detected in deposits from 100% CCP cases, particularly potassium, will be discussed in the subsection dedicated to
 337 ESEM analyses (see 3.2.2.1).

338



339 **Fig. 8. Images of ash deposits formed on the probes: (a) Air-firing 100% EC; (b) Air-firing 50% EC-50% CCP; (c) Air-firing 100%**
 340 **CCP; (d) Oxy-firing 100% EC; (e) Oxy-firing 50% EC-50% CCP; (f) Oxy-firing 100% CCP**

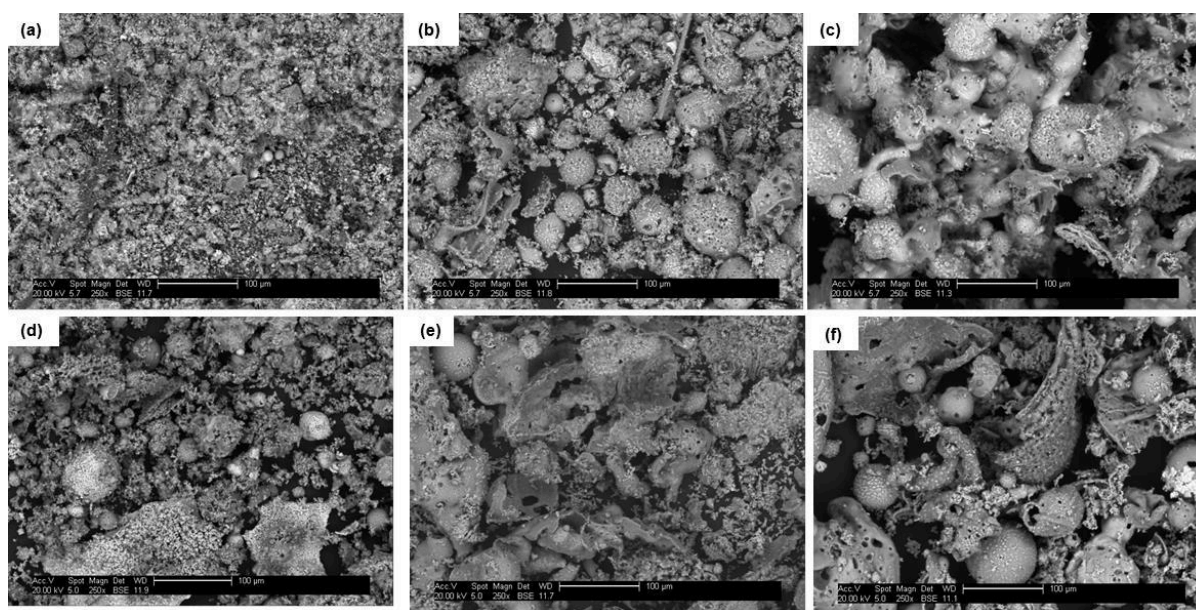
341 It was also noted that the unburnt carbon contents of the deposit samples taken from the deposition probes showed
 342 100% burn-out for all the cases: air and oxy-firing.

343

3.2.2.1 ESEM/EDX analyses

344 Fig. 9 presents the micrographs (at the same magnification) generated for different deposit samples during the
 345 ESEM/EDX analyses. These images show the differences in particle sizes found between the ash deposits when
 346 varying the fuel blend and when changing the type of firing mode from air to oxy-firing. The most perceptible effect
 347 is the increasing deposit particle size with increasing levels of CCP, for both air-firing and oxy-firing. The more
 348 fibrous appearance for the cases with higher shares of biomass can also be observed, reflecting the biomass cellulose
 349 structure. These fibres are mostly rich in Si, but sometimes appear together with K or Ca. The rounded/spherical
 350 particles with surface pores shown in the images are the result of ash melting and expansion of gas evolution from the
 351 residual carbon-rich material. These are greater for the higher share of CCP as a consequence of the lower ash fusion
 352 temperatures comprising high contents of Si and K, along with P or S levels in some particles. In all cases it should be
 353 expected that these particles contain largely amorphous material from the partial decomposition of the minerals in the

354 fuels and from vapour phase species, as few crystalline particles can be seen, consistent with fly ashes and ash
355 deposits from other combustion processes.

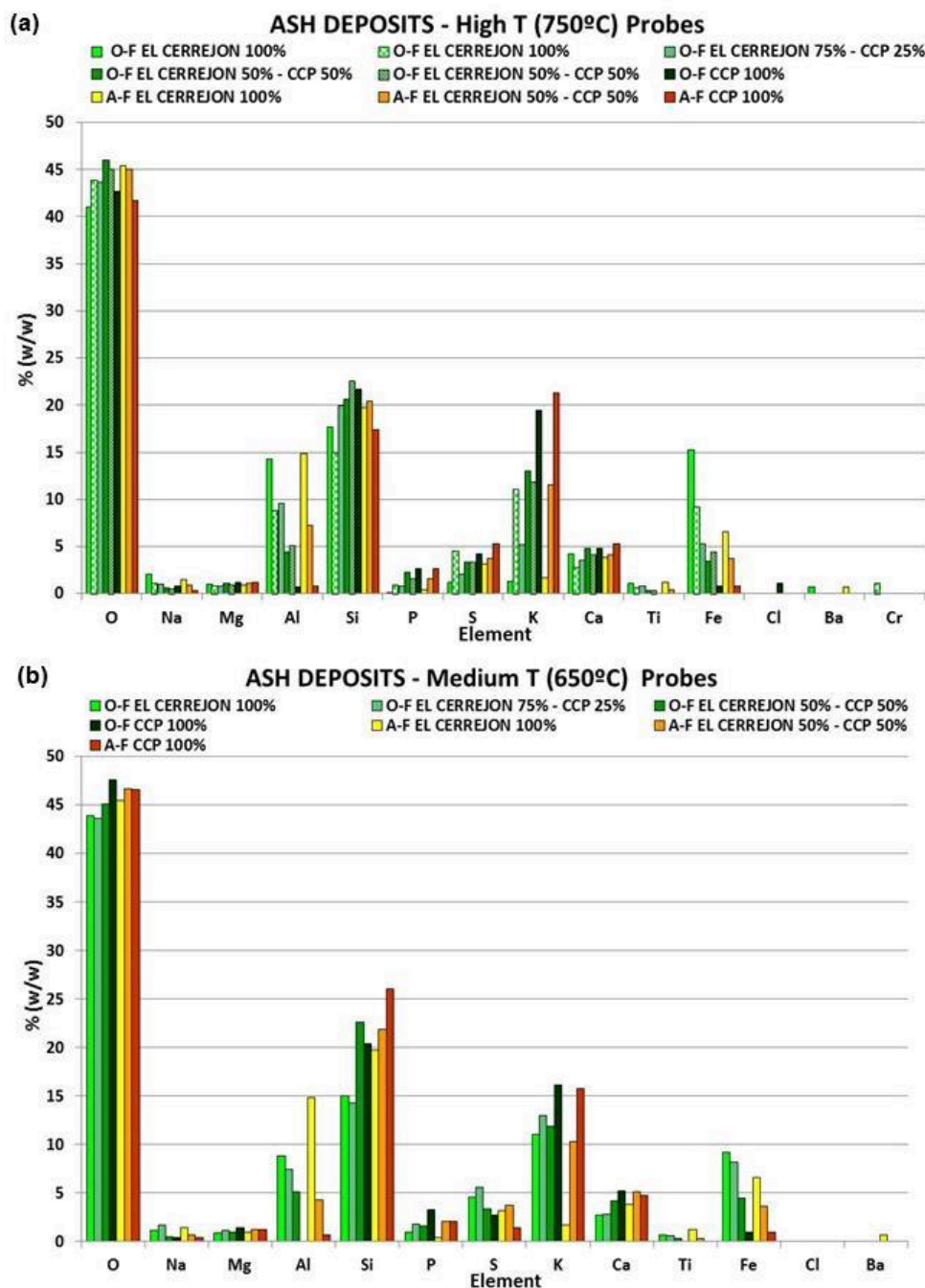


356
357 **Fig. 9. ESEM images: (a) Air-firing 100% EC; (b) Air-firing 50% EC-50% CCP; (c) Air-firing 100% CCP; (d) Oxy-firing 100%**
358 **EC; (e) Oxy-firing 50% EC-50% CCP; (f) Oxy-firing 100% CCP**

359 Results from the ESEM/EDX analyses of the deposits are shown in Fig. 10. The reference considered to evaluate
360 these results is the mineral and the ash analyses of the parent fuels presented in Table 1. The ESEM/EDX results for
361 the deposits sampled at high temperature (~750°C) are presented in Fig. 10(a). The majority of the elements detected
362 follow the trends shown in the fuel ash analyses, with a tendency for Na, Al, Ti and Fe to increase with the share of
363 EC in the fuel blend. On the other hand, the contents of Mg, P, K, Ca and Cl increase with the share of biomass used.
364 For the particular case of P, this trend is less marked than might have been expected from the ash analyses of the
365 parent fuels, but this is consistent with experience of phosphates condensing to form adherent deposits on lower-
366 temperature surfaces (e.g., economisers) further along the flue gas path. It is interesting to note the low K contents
367 obtained for the tests using 100% EC, consistent with the fact that, generally, in coals, this element is mostly present
368 in clay minerals (e.g. illite), restricting its release as vapour-phase K species (higher temperatures are required to
369 release K from illite). This is contrary to what happens in the case of biomass where the K is not bound in clay
370 minerals, but is rather in an organic form from which it is easily released. The two elements that do not show clear
371 patterns are Si and S. The Si contents are similar for all the cases reported, even though it should be higher for those
372 cases with greater share of EC on a law of mixtures basis. The tests with maximum Si levels are those using the coal-
373 biomass blend 50% EC-50% CCP, and 100% CCP. An interesting ratio to examine is that between aluminium and
374 silicon. The Al/Si ratios detected for cases using coal-biomass blends and pure biomass correspond to the ratios in the
375 parent fuels presented in Table 1. However, the Al/Si ratio resulting for the cases using 100% EC, under air and oxy-
376 firing, is twice the value of the ratio expected. For the S content, similar values are observed when using pure biomass
377 or coal, even though the ultimate analysis, presented in Table 1, shows that EC has 3.5 times more sulphur than CCP.
378 This fact may be due to the retention of sulphur in the ash deposits by the potassium, present to a greater extent in the
379 biomass, leading to higher levels of K₂SO₄ in the high-CCP blend deposits. This assumption will be justified in the
380 following subsection (3.2.2.2), where the results from the XRD analyses are presented, giving details about the
381 compounds present in the ash deposits.

382 Fig. 10(b) presents the results of the ESEM/EDX analyses of the ashes sampled at medium temperature (~650°C).
383 The observations made for the deposits at high temperature (~750°C) are repeated, in general, for the results at
384 medium temperature, although some additional remarks must be made for Al/Si ratios and S. For the Al/Si ratios,
385 similar to the results reported for high temperature, only the cases using coal-biomass blends and pure biomass kept
386 the Al/Si ratios shown in the parent fuels ash analyses in Table 1. The S levels show a maximum for the tests using
387 coal-biomass blends, and a minimum when using 100% CCP. However, the levels reached for the tests with 100%
388 CCP are still higher than expected considering the ultimate analyses of the parent fuels; the most probable explanation

389 for this is K_2SO_4 formation, already discussed above. These aspects were observed for both firing modes: air and oxy-
 390 firing.



391
 392

Fig. 10. Elemental analyses of deposits sampled at: (a) 750°C; (b) 650°C, varying fuel and firing mode.

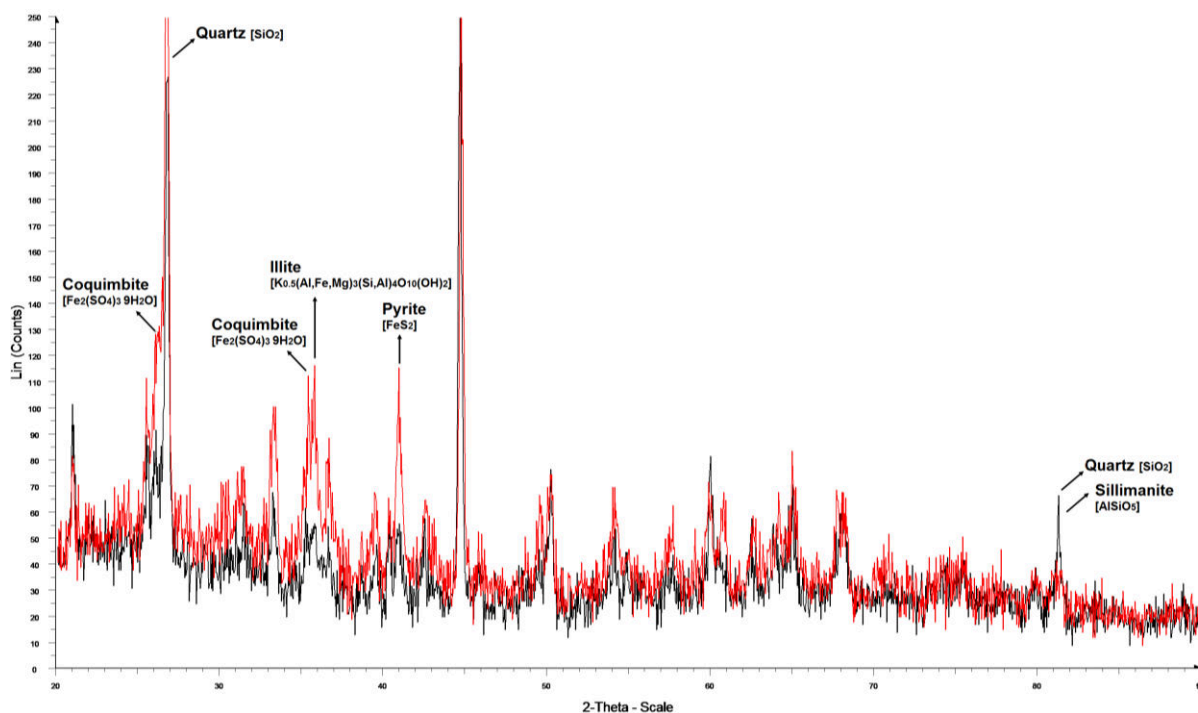
393 More details on the data obtained during this experimental work, such as temperature profiles inside the
 394 combustion chamber or heat fluxes, can be found in a previous publication [8].

395 **3.2.2.2 XRD analyses**

396 For the evaluation of the XRD results, comparisons have been made to get a better understanding of how a change
 397 in fuel blend and/or the firing mode affect the composition of the ash deposits. Air and oxy-firing were, therefore,
 398 compared for a given type of fuel. Comparison was also made between results generated when the fuel was varied
 399 from 100% coal to 100% biomass for a given combustion mode.

400 For the case using 100% EC, the patterns generated for deposits sampled under air-firing (black) and under oxy-
 401 firing conditions (red) are illustrated in Fig. 11. The peaks corresponding to crystalline compounds observed as

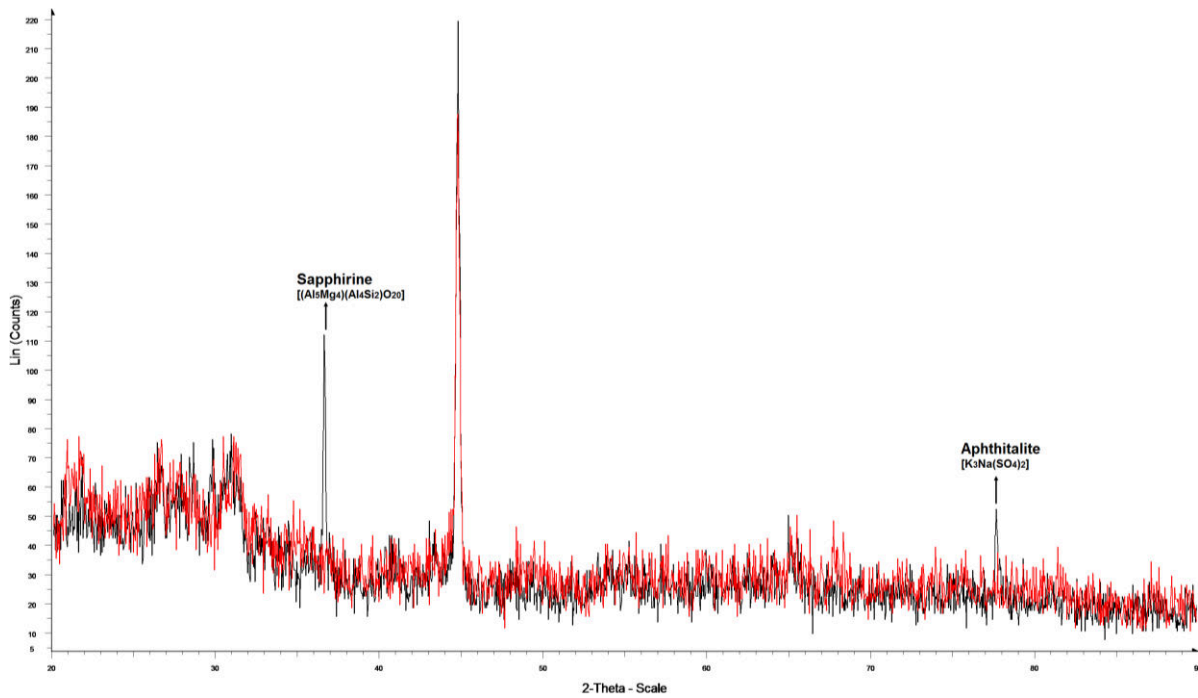
402 different between the two cases are highlighted and labelled in the graph. However, the high background level shown
 403 is consistent with most of the material being amorphous in the samples analysed, as observed in the ESEM
 404 micrographs presented earlier, and so the crystalline phases identified represent only minor species in the deposits and
 405 may not be of real significance. This phenomenon is more important for the cases evaluating biomass ash, as they
 406 have been reported to have a greater non-crystalline character compared to coal ash [29]. Under oxy-firing conditions
 407 using 100% coal, crystalline compounds such as quartz, coquimbite, illite and pyrite are found at higher levels than in
 408 the air-firing case. Quartz is often found in ash and deposit samples and is of little significance as very small amounts
 409 can show in XRD analysis. The presence of the clay mineral illite and pyrites, along with the partially oxidised Fe/S
 410 compound coquimbite, are surprising and suggest that some ash particles reached the deposit probes either during or
 411 after the tests without having been through a high-temperature flame; illite particles would normally be expected to
 412 have been transformed into an amorphous alumina-silicate phase, and pyrites into an Fe oxide if they had reached
 413 flame temperatures heated during combustion. Also, the presence of fluid matter as a mineralised aqueous solution
 414 (e.g., coquimbite) is expected in those cases analysing biomass ash but it is more unusual when looking at coal ash,
 415 according to Vassilev et al. [29]. The only compound found at higher concentration in air combustion was sillimanite
 416 (an alumino-silicate) which is derived during the decomposition of clay minerals (such as kaolinite which transforms
 417 and recrystallizes more readily than illite).



418

419 **Fig. 11. XRD charts for EC ashes collected at 640-700°C: air-firing (black spectrum) vs. oxy-firing (red spectrum)**

420 For the case using 50% EC-50% CCP, the spectra generated for ashes sampled under air-firing (red) and under
 421 oxy-firing conditions (black) are illustrated in Fig. 12 (the colours in this figure and in Fig 13 are reversed from those
 422 in Fig 11). There are fewer crystalline compounds to be seen in this case, indicating that a higher proportion of the
 423 deposit material is amorphous, in accordance with the view that biomass ash has a marked non-crystalline character
 424 [29]. Those peaks found relate to minor amounts of sapphirine (a silicate of magnesium and aluminium) and
 425 apthitalite (a potassium sulphate mineral) under oxy-firing conditions. The sulphates and silicates found in this
 426 instance are in agreement with the classification given by Vassilev et al. [4] where coal ash is expected to present
 427 higher levels of these species.



428

429

Fig. 12. XRD charts for 50% EC -50% CCP ashes collected at 610-650°C: air-firing (red spectrum) vs. oxy-firing (black spectrum)

430

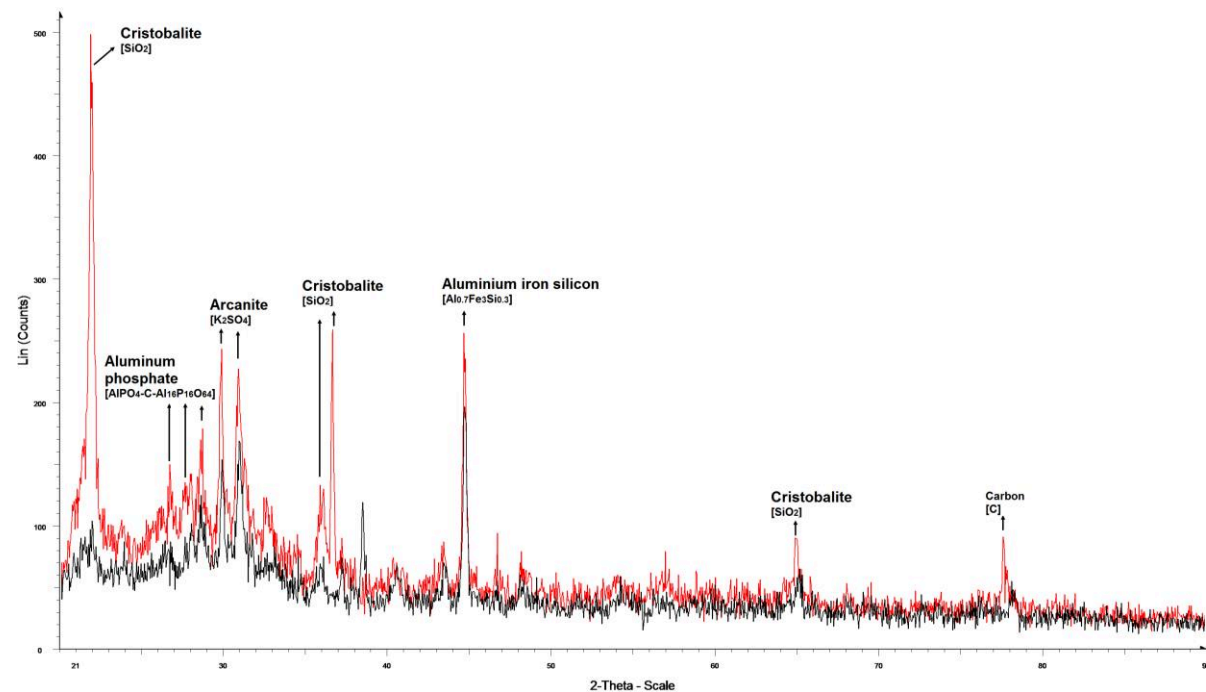
431

432

433

434

435



436

437

Fig. 13. XRD charts for 100% CCP ashes collected at 650-680°C: air-firing (red spectrum) vs. oxy-firing (black spectrum)

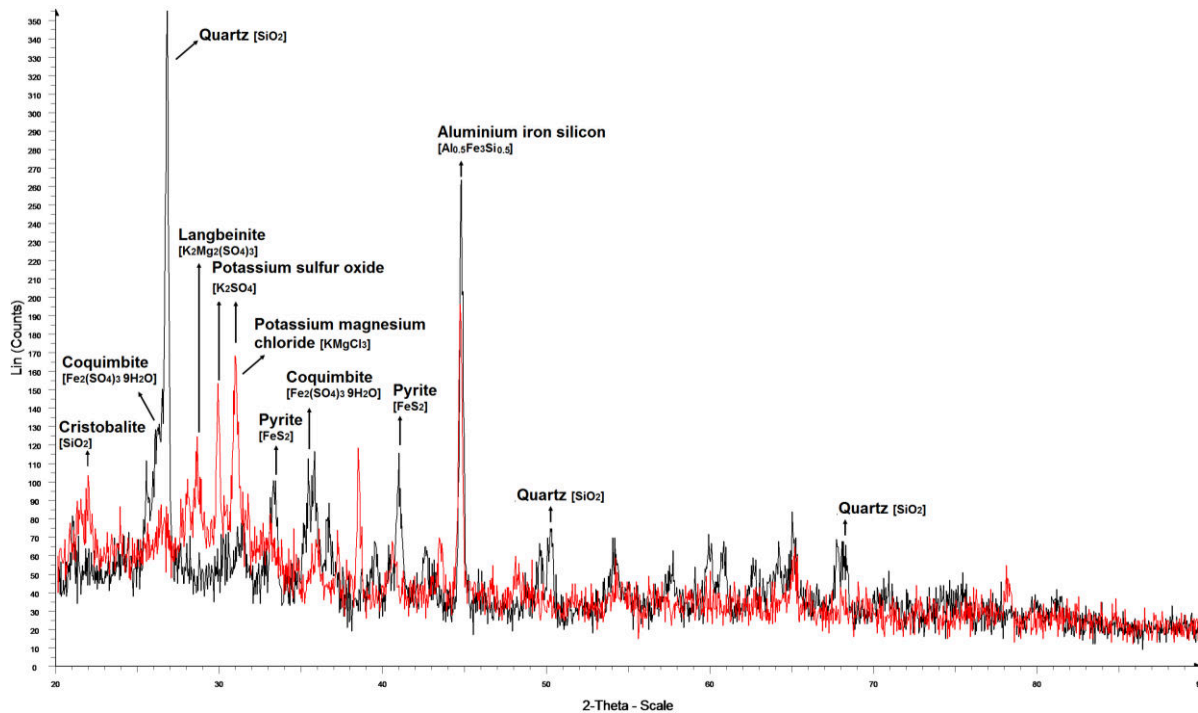
438

439

440

For the comparison of the results obtained for 100% EC and 100% CCP under oxy-firing conditions, the corresponding spectra are presented in Fig. 14. From this figure, it can be seen that crystalline compounds such as quartz (SiO_2), aluminium-iron-silicon, coquimbite and pyrite are dominant for ashes generated when oxy-firing 100%

441 EC, which is compatible with the expected components for coal ash according to the relevant literature [4]; this also
442 indicates incomplete transformation of the coal minerals as suggested above. On the other hand, when using 100%
443 CCP, cristobalite (a high-temperature form of SiO₂), potassium sulphur oxide (K₂SO₄) and potassium magnesium
444 chloride (KMgCl₂) were found, fully consistent with the composition of CCP ash.



445
446 Fig. 14. XRD charts for oxy-firing ashes collected at 680-700°C: 100% EC (black spectrum) vs. 100% CCP (red spectrum)

447 4. Discussion of findings and technological implications

448 The series of pilot-scale tests carried out co-firing a biomass feedstock (CCP) with addition of 0, 50, 75 and 100%
449 (w/w) of EC under air and oxy-firing conditions have provided new information on the gaseous environments the
450 compositions and characteristics of the fly ash and ash deposits formed on air-cooled deposit probes with surface
451 temperatures in the range from 650 to 750°C (to simulate operating temperatures similar to those reached by
452 superheaters/reheaters at industrial-scale facilities).

453 It was found that similar CO₂ levels can be reached, on a dry basis, using 100% coal or 100% biomass. The H₂O
454 levels measured in oxy-combustion tests with no flue gas treatment prior to gas recycle showed concentrations up
455 to three times higher than in combustion with air. As expected, the flue gas generated using a high share of biomass
456 (without any flue gas treatment prior to recycle) will have higher H₂O content, as a consequence of the higher H₂ and
457 O₂ concentrations of the biomass. The presence of this additional H₂O needs to be considered when designing the flue
458 gas recycle system to avoid acid dew point corrosion problems in the recycle gas path when using blends with high
459 biomass content.

460 The main difference between air and oxy-combustion was the increase in the SO₂ content, which was up to 2.6
461 times higher when using coal in oxy-combustion compared to the same case under air-firing conditions (without
462 considering normalisation per unit of energy released from the fuel); this is a direct consequence of the recycle of
463 those species which are not removed before re-injection of the flue gas into the combustor. With an increasing
464 share of biomass in the fuel blend, the SO₂ levels decreased while HCl levels increased, as expected from the ultimate
465 analysis of the parent fuels. No significant variations in the NO_x levels were found with changed levels of biomass,
466 except for the 50/50 blend, where high levels of excess oxygen were supplied (~6% (v/v)), causing an increase in the
467 NO_x generation from the fuel-N (biomass presents higher N contents than coal in its ultimate analysis). Additionally,
468 it has been described when analysing the effect of the firing mode, air vs. oxy, on the emissions generated, that the
469 presence of SO₂ and NO_x in the flue gas must be evaluated on the basis of normalised results; by doing this, the results
470 showed a decrease in the levels of SO₂ and NO_x under oxy-firing conditions, a fact that is consistent with findings
471 from other researchers [6,17,28]. The effect of the type of recycle (wet vs. dry), revealed increases in the

472 concentrations reached for all species except steam, as expected. The minor species NO_x and SO₂ were found to be
473 especially sensitive to this change.

474 While the results for the carbon in ash were not fully consistent, elevated levels were observed in the air-firing
475 cases compared to oxy-firing, where the combustion process is assumed to be enhanced by the higher O₂
476 concentrations and higher temperatures reached. However, no clear trend was found by varying the type of fuel.

477 The other major aspect of the study was to investigate ash deposition with respect to the relative risks of fouling
478 and corrosion in oxy-firing and when a high share of biomass was used in the fuel blend. The extent of deposition
479 increased with an increasing share of biomass, but did not show any perceptible change between air- and oxy-firing;
480 and so similar measures (e.g., soot blowers) to restrict the build-up of ash deposits should be applicable. Larger
481 particles were found in the deposits generated using pure biomass, without showing noticeable differences when
482 varying the firing mode.

483 The deposit compositions showed similar patterns at high (750°C) and medium (650°C) deposition temperatures,
484 where most of the elements followed the trend demonstrated by the fuel analyses. The main exception found to these
485 trends was for S, as similar S levels were found in all cases, even though EC has 3.5 times more S than CCP. This is
486 consistent with the higher K levels contained in the biomass leading to much greater formation and deposition of
487 K₂SO₄. The low K contents obtained for cases using EC are consistent with the fact that this element tends to be
488 mixed with the clay present in coals, limiting its release. Cl was detected in the ash deposits for the cases using pure
489 biomass under oxy-firing conditions. The higher levels of S and Cl in deposits when 100% CCP was fired were
490 confirmed by the XRD analyses which, under air-firing conditions showed the presence of arcanite (K₂SO₄) as well as
491 an indication of the presence of potassium magnesium chloride. The presence of sulphate and, in particular, chloride
492 species in the deposits are a concern with respect to fireside corrosion [5], although both species are routinely found in
493 deposits in biomass boilers. In these systems, efforts are made to minimise the presence of chloride species which lead
494 to the very aggressive corrosion mechanisms found in waste incineration and to reduce the plant's steam parameters,
495 and hence superheater/reheater metal temperatures to obtain economically viable component lives. Fireside corrosion
496 risks [5] in these systems increase with higher fluxes of sulphate species in the deposits formed, and so similar
497 measures can be used to address these risks in both air- and oxy-firing systems using high shares of biomass.

498 **Conclusions**

499 The experimental study of the co-firing of coal and biomass under air- and oxy-firing conditions has generated new
500 information on the gaseous environments prevailing in the combustion gas path and on the deposition behaviour of the
501 ash. While the study has been limited to one type of coal and one type of biomass, it has provided clear information in
502 support of the view that experience from air-firing can be readily translated to oxy-firing systems with reasonable
503 confidence. Ash deposition behaviour was found to be similar in both air- and oxy-firing, indicating that similar
504 approaches to handle ash fouling and fireside corrosion can be used in both cases. Studies with other coals and
505 biomass fuels are required to ensure that this conclusion can be applied widely.

506 **Acknowledgements**

507 The authors gratefully acknowledge the E.ON and UK Engineering and Physical Sciences Research Council
508 (EPSRC) funding and lead via the Oxyfuel Combustion - Academic Programme for the UK (OxyCAP) Consortium.
509 The authors would also like to thank Dr. Mohamad J Al-Jeboori and Dr Paul Fennell from Imperial College London
510 for their help with the analyses of size distribution of the fuels used for this work.

511 **References**

- 512 [1] International Energy Agency. CO₂ Emissions From Fuel Combustion Highlights. IEA Statistics 2013:158. doi:10.1787/co2-table-
513 2011-1-en.
- 514 [2] UK Parliament. Climate Change Act 2008 2008:1–103. doi:10.1136/bmj.39469.569815.47.
- 515 [3] Adams D. Flue gas treatment for CO₂ capture. Report CCC/169 IEA Clean Coal Centre. ISBN 978-92-9029-489-4. 2010.

- 516 [4] Vassilev S V., Vassileva CG, Vassilev VS. Advantages and disadvantages of composition and properties of biomass in
517 comparison with coal: An overview. *Fuel* 2015;158:330–50. doi:10.1016/j.fuel.2015.05.050.
- 518 [5] Arias B, Pevida C, Rubiera F, Pis JJ. Effect of biomass blending on coal ignition and burnout during oxy-fuel combustion. *Fuel*
519 2008;87:2753–9. doi:10.1016/j.fuel.2008.01.020.
- 520 [6] Toftegaard MB, Brix J, Jensen P a., Glarborg P, Jensen AD. Oxy-fuel combustion of solid fuels. *Progress in Energy and*
521 *Combustion Science* 2010;36:581–625. doi:10.1016/j.pecs.2010.02.001.
- 522 [7] Smart JP, Patel R, Riley GS. Oxy-fuel combustion of coal and biomass, the effect on radiative and convective heat transfer and
523 burnout. *Combustion and Flame* 2010;157:2230–40. doi:10.1016/j.combustflame.2010.07.013.
- 524 [8] Jurado N, Darabkhani HG, Anthony EJ, Oakey JE. Oxy-combustion Studies Into the Co –Firing of Coal and Biomass Blends:
525 Effects on Heat Transfer, Gas and Ash Compositions. *Energy Procedia* 2014;63:440–52. doi:10.1016/j.egypro.2014.11.047.
- 526 [9] Syed AU, Simms NJ, Oakey JE. Fireside corrosion of superheaters: Effects of air and oxy-firing of coal and biomass. *Fuel*
527 2012;101:62–73. doi:10.1016/j.fuel.2011.03.010.
- 528 [10] Khodier A, Simms N. Investigation of gaseous emissions and ash deposition in a pilot-scale PF combustor co-firing cereal co-
529 product biomass with coal. *Conference on Renewable Energies and Power Quality* 2010.
- 530 [11] Bartolomé C, Gil A, Ramos I. Ash deposition behavior of cynara–coal blends in a PF pilot furnace. *Fuel Processing Technology*
531 2010;91:1576–84. doi:10.1016/j.fuproc.2010.06.005.
- 532 [12] Chen L, Yong SZ, Ghoniem AF. Oxy-fuel combustion of pulverized coal: Characterization, fundamentals, stabilization and CFD
533 modeling. *Progress in Energy and Combustion Science* 2012;38:156–214. doi:10.1016/j.pecs.2011.09.003.
- 534 [13] Galloway BD, Sasmaz E, Padak B. Binding of SO₃ to fly ash components: CaO, MgO, Na₂O and K₂O. *Fuel* 2015;145:79–83.
535 doi:10.1016/j.fuel.2014.12.046.
- 536 [14] Jiménez S, Ballester J. Effect of co-firing on the properties of submicron aerosols from biomass combustion. *Proceedings of the*
537 *Combustion Institute* 2005;30:2965–72. doi:10.1016/j.proci.2004.08.099.
- 538 [15] Valmari T. Potassium behaviour during combustion of wood in circulating fluidised bed power plants. *VTT Publications* 2000.
- 539 [16] Kassman H, Bäfver L, Åmand LE. The importance of SO₂ and SO₃ for sulphation of gaseous KCl - An experimental
540 investigation in a biomass fired CFB boiler. *Combustion and Flame* 2010;157:1649–57. doi:10.1016/j.combustflame.2010.05.012.
- 541 [17] Spörl R, Maier J, Scheffknecht G. Sulphur Oxide Emissions from Dust-fired Oxy-fuel Combustion of Coal. *Energy Procedia*
542 2013;37:1435–47. doi:10.1016/j.egypro.2013.06.019.
- 543 [18] Li W, Wang L, Qiao Y, Lin J-Y, Wang M, Chang L. Effect of atmosphere on the release behavior of alkali and alkaline earth
544 metals during coal oxy-fuel combustion. *Fuel* 2015;139:164–70. doi:10.1016/j.fuel.2014.08.056.
- 545 [19] Hussain T, Khodier AHM, Simms NJ. Co-combustion of cereal co-product (CCP) with a UK coal (Daw Mill): Combustion gas
546 composition and deposition. *Fuel* 2013;112:572–83. doi:10.1016/j.fuel.2013.01.001.
- 547 [20] Santisteban J, Mediavilla R, López-Pamo E, Dabrio CJ, Ruiz Zapata MB, García MJG, et al. Loss on ignition: a qualitative or
548 quantitative method for organic matter and carbonate mineral content in sediments? *Journal of Paleolimnology* 2004;32:287–99.
- 549 [21] Vassilev S V., Vassileva CG. Methods for Characterization of Composition of Fly Ashes from Coal-Fired Power Stations: A
550 Critical Overview. *Energy & Fuels* 2005;19:1084–98. doi:10.1021/ef049694d.
- 551 [22] Fan M, Brown RC. Comparison of the Loss-on-Ignition and Thermogravimetric Analysis Techniques in Measuring Unburned
552 Carbon in Coal Fly Ash. *Energy & Fuels* 2001;15:1414–7. doi:10.1021/ef0100496.
- 553 [23] Zhao M, Han Z, Sheng C, Wu H. Characterization of Residual Carbon in Fly Ashes from Power Plants Firing Biomass. *Energy &*
554 *Fuels* 2013;27:898–907. doi:10.1021/ef301715p.
- 555 [24] Wigley F. Coal mineral transformations under oxy-fuel combustion conditions Final report for BCURA Project B81 (1 January
556 2007 – 30 September 2009). vol. 81. 2010.
- 557 [25] Riaza J, Álvarez L, Gil MV, Pevida C, Pis JJ, Rubiera F. Ignition and NO Emissions of Coal and Biomass Blends under Different
558 Oxy-fuel Atmospheres. *Energy Procedia* 2013;37:1405–12. doi:10.1016/j.egypro.2013.06.016.

- 559 [26] Pawlak-Kruczek H, Ostrycharczyk M, Baranowski M, Czerep M, Zgóra J. Co-Firing of Biomass with Pulverised Coal in Oxygen
560 Enriched Atmosphere. *Chemical and Process Engineering* 2013;34:215–26. doi:10.2478/cpe-2013-0018.
- 561 [27] Buhre BJP, Elliott LK, Sheng CD, Gupta RP, Wall TF. Oxy-fuel combustion technology for coal-fired power generation. *Progress*
562 *in Energy and Combustion Science* 2005;31:283–307. doi:10.1016/j.pecs.2005.07.001.
- 563 [28] Fleig D, Andersson K, Johnsson F, Leckner B. Conversion of sulfur during pulverized oxy-coal combustion. *Energy and Fuels*
564 2011;25:647–55. doi:10.1021/ef1013242.
- 565 [29] Vassilev S V., Baxter D, Andersen LK, Vassileva CG. An overview of the composition and application of biomass ash. Part 1.
566 Phase-mineral and chemical composition and classification. *Fuel* 2013;105:40–76. doi:10.1016/j.fuel.2012.09.041.

567